

## Thermodynamics of Water Entry in Hydrophobic Channels of Carbon Nanotubes

Hemant Kumar and Biswaroop Mukherjee

*Centre For Condensed Matter Theory, Department of Physics,  
Indian Institute of Science, Bangalore, 560 012, India*

Shiang-Tai Lin

*Department of Chemical Engineering, National Taiwan University, Taipei, 10617,  
Taiwan*

Chandan Dasgupta

*Centre For Condensed Matter Theory, Department of Physics,  
Indian Institute of Science, Bangalore, 560 012, India*

A.K. Sood

*Department of Physics, Indian Institute of Science, Bangalore, 560012,  
India*

Prabal K. Maiti

*Centre For Condensed Matter Theory, Department of Physics,  
Indian Institute of Science, Bangalore, 560 012, India<sup>a)</sup>*

(Dated: 13 November 2018)

Experiments and computer simulations demonstrate that water spontaneously fills the hydrophobic cavity of a carbon nanotube. To gain a quantitative thermodynamic understanding of this phenomenon, we use the recently developed Two Phase Thermodynamics (2PT) method to compute translational and rotational entropies of confined water molecules inside single-walled carbon nanotubes and show that the increase in energy of a water molecule inside the nanotube is compensated by the gain in its rotational entropy. The confined water is in equilibrium with the bulk water and the Helmholtz free energy per water molecule of confined water is the same as that in the bulk within the accuracy of the simulation results. A comparison of translational and rotational spectra of water molecules confined in carbon nanotubes with that of bulk water shows significant shifts in the positions of the spectral peaks that are directly related to the tube radius.

---

<sup>a)</sup>Electronic mail: maiti@physics.iisc.ernet.in

## I. INTRODUCTION

Understanding the properties of water confined in a one-dimensional channel of diameter comparable to a few molecular diameters is important in many technological and biological processes. Such strong confinement leads to dramatic changes in the structure and dynamics of water. An ideal system for studying such confinement effects is water inside single-walled carbon nanotubes (SWCNT). Several simulations and some experiments have demonstrated that water spontaneously fills up the hydrophobic pore of a nanotube when it is immersed in a bath of water<sup>1,2,7,8</sup>. Hummer *et al.*<sup>1</sup> demonstrated for the first time, via classical molecular dynamics (MD) simulations, that narrow (6,6) SWCNTs immersed in a bath of water remain filled with water molecules throughout simulation run times of up to 66 ns. The single-file chain of water molecules exhibits rapid concerted movements along the axis of the tube. The hydrogen bond network of water molecules inside a narrow nanotube is very different from that of bulk water: the number of hydrogen bonded neighbors of a water molecule inside a narrow nanotube is generally smaller than that in the bulk. This causes the hydrogen bonding energy of water molecules inside a nanotube to be higher than that of water molecules in the bulk. The increase in the hydrogen bonding energy of water molecules inside a (6,6) nanotube is about 10 kcal/mol, of which only about 6 kcal/mol can be recovered from their interactions with the carbon atoms. Therefore, considering the energetics, it is surprising that water molecules spontaneously fill up the nanotube. Although there have been attempts to understand thermodynamics of entry of water molecules in the hydrophobic pore of a narrow nanotube, it is still not well understood. Maibun *et. al.*<sup>3</sup> and Zhou *et. al.*<sup>4</sup> have explained filling and emptying transition in hydrophobic channels using a lattice-gas model. Vaitheeswaran *et. al.*<sup>6</sup> have calculated free energy of transfer for water molecules, from bulk to carbon nanotube channel for different occupancy of nanotube, using statistical-mechanical framework for the periodically replicated nanotubes. They have computed free energy of transfer for the water molecules in 13.4Å long nanotube with diameter 8.1Å in virtual equilibrium with bulk water, for the various occupancy and shown N=6 is most stable filling for this nanotube. In an excellent review rasaiah *et. al.*<sup>5</sup> have reviewed thermodynamic, structural and kinetic aspects of water in various kind of confinement including CNT, protein cavity and flurene. Despite all these attempts, fully microscopic description for this phenomenon is not well understood. This is generally

attributed<sup>1</sup> to the rotational entropy gained by the water molecules on entering the tube, a suggestion which has not been verified quantitatively so far.

Detailed information about the rotational dynamics of water molecules inside narrow carbon nanotubes is necessary for understanding the role of rotational entropy in the thermodynamics of entry of water molecules in a nanotube. Earlier studies<sup>9,10</sup> have shown that water molecules confined inside a (6,6) nanotube form an orientationally ordered chain with the dipole moments of the water molecules pointing either parallel or anti-parallel to the axis of the tube (see Fig.1). Occasionally, there are orientational defects in the chain, where the water molecule points perpendicular to the chain. As shown in Fig. 1, each water molecule in the chain is hydrogen bonded to two water molecules, one in front and the other behind it. This arrangement of molecules leaves one hydrogen atom for each water molecule free which does not participate in any hydrogen bond. The altered hydrogen bond network severely modifies the orientational dynamics<sup>9</sup> of the confined water molecules. The orientational relaxation of the confined water molecules is found to occur in several different time scales and it also exhibits a strong directional anisotropy. The slowest relaxation is that of the collective dipole moment (time scale of several nanoseconds). This relaxation is mediated by orientational defects in the hydrogen-bonded chain: a transition from the parallel to the anti-parallel (or vice versa) state occurs when a defect is able to hop across the whole chain. Since the creation of a defect is energetically unfavorable, collective flips of the dipole moment occur rarely (on a time scale of nanoseconds). On the other hand, the relaxation of the vector joining the hydrogen atoms (HH vector) of each confined water molecule is much faster (with a time scale of about 200fs) than that of water molecules in the bulk. Maintaining the hydrogen bond network of two hydrogen bonds per water molecule, the HH vector can rotate easily about the common dipolar direction in the cylindrically symmetric environment provided by the neutral carbon atoms of the nanotube. In addition, the water molecules exhibit another rotational mode, where there is a fast (time scale of about 60 fs) exchange of the positions of the hydrogen atom participating in the hydrogen bonding in the chain and the one that is free. This exchange is by a non-diffusive angular jump, where the mean jump angle is about 50 degrees<sup>11</sup> and the mean waiting time between successive jumps is about 1 ps. The orientational relaxation of water molecules in the bulk is also known to involve large amplitude angular jumps<sup>12</sup>. In the bulk, the waiting time between two successive jumps is about 2 ps, which is slightly reduced in the case of water in nanotubes due to

strong confinement. Hummer *et al.*<sup>1</sup> have commented that despite strong hydrophobic confinement, the single-file water molecules retain considerable orientational freedom resulting in a highly degenerate state with a narrow energy distribution. The reorientational processes described above provide a clear microscopic picture of the "degenerate states" involved in the orientational relaxation.

In the present study, we investigate how the presence of these microscopic degenerate states affects the thermodynamics of water occupancy of the narrow hydrophobic pores of carbon nanotubes. We present the results of a numerical calculation of the entropy and free energy of water molecules using trajectories obtained from atomistic MD simulations. For the computation of the entropy of bulk and confined water, we have used the 2PT method of Lin *et al.*<sup>13</sup>. This is a modification of the quasi-harmonic approximation method where the entropy is determined by treating each mode in the vibrational spectrum as a harmonic oscillator. In the present 2PT method, anharmonic effects have been explicitly included. It has been demonstrated<sup>13</sup> that this method yields accurate estimates of thermodynamic quantities from reasonably short MD trajectories (several tens of picoseconds). Earlier, the 2PT scheme was successfully used for calculating the entropy of water in different domains of PAMAM dendrimers<sup>14</sup>, for determining various phases of dendrimer liquid crystals<sup>15</sup> and in calculating the relative stability of various forms of aggregates<sup>15</sup>. More recently, it has also been used to compute the entropy of water molecules in major and minor grooves of DNA<sup>16</sup>, showing that the entropies are significantly lower than that in bulk water. In this paper, we compute the entropy of water molecules confined in SWCNTs of various diameters ranging from 6.9 Å to 10.8 Å (in standard nomenclature, (5,5) to (8,8)), where water molecules are organized in different geometrical arrangement. In all cases, we find that the confined water molecules have more rotational entropy than the water molecules in the bulk, the difference being maximum for molecules inside the narrowest (5,5) nanotubes. The interaction energy of each water molecule has also been computed, from which we were able to calculate the average Helmholtz free energy ( $F = E - TS$ ). We find that in all cases except (5,5) nanotubes, the free energy of a water molecule in the bulk is the same as its free energy under confinement, within the accuracy of our calculation. For water molecules inside a (5,5) SWCNT (diameter 6.9Å) the gain in entropy is not able to compensate the increase in energy. This results in reduced occupation of the nanotube by water molecules.

The rest of the article is arranged as follows. In the next section II, we provide the

theoretical details of the 2PT method. Section III describes the simulation method and the results are described in detail in section IV. Section V contains a summary of our main conclusions.

## II. TWO PHASE THERMODYNAMICS METHOD

The translational density of states (DoS) for solids represents the phonon spectrum<sup>17</sup> as in the Debye-Einstein Model. Thermodynamic quantities for solids can be computed by treating the phonon modes as a system of non-interacting harmonic oscillators. Hard sphere fluids have exponentially decaying velocity auto-correlation function, within low density approximation<sup>17</sup>, hence DoS function can be extracted analytically. The 2PT method is based on the premise that a fluid can be regarded as a two component system consisting of solid and gas. Based on this premise, Lin *et al.*<sup>13</sup> suggested that thermodynamic properties of fluids can be computed by treating the DoS of fluids as a sum of solid-like [ $S^s(\nu)$ ] and gas-like [ $S^g(\nu)$ ] contributions. Using this prescription, they have computed very accurate thermodynamic quantities of Lennard-Jones fluids over a wide range of thermodynamic state points from the DoS function obtained from only 20ps MD trajectory. The translational density of states  $S(\nu)$  of a system is defined as the mass-weighted sum of atomic spectral densities  $s_j^k(\nu)$ ,

$$S(\nu) = \frac{2}{k_B T} \sum_{j=1}^N \sum_{k=1}^3 m_j s_j^k(\nu), \quad (1)$$

where  $m_j$  is the mass of the  $j^{\text{th}}$  atom,  $k$  refers to Cartesian directions  $x, y, z$ , and  $s_j^k(\nu)$  is defined as

$$s_j^k(\nu) = \lim_{\tau \rightarrow \infty} \frac{|\int_{-\tau}^{\tau} v_j^k(t) e^{-i2\pi\nu t} dt|^2}{\int_{-\tau}^{\tau} dt} \quad (2)$$

where  $v_j^k(t)$  is the  $k^{\text{th}}$  component of the velocity of atom  $j$ . It can be shown that the atomic spectral density defined as above can be obtained from the Fourier transform of the velocity auto-correlation function (VACF)  $c_j^k(t)$ <sup>13</sup>:

$$s_j^k(\nu) = \lim_{\tau \rightarrow \infty} \int_{-\tau}^{\tau} c_j^k(t) e^{-i2\pi\nu t} dt. \quad (3)$$

Therefore, Eq.(1) can be rewritten as

$$S(\nu) = \frac{2}{k_B T} \lim_{\tau \rightarrow \infty} \int_{-\tau}^{\tau} \sum_{j=1}^N \sum_{k=1}^3 m_j c_j^k(t) e^{-i2\pi\nu t} dt. \quad (4)$$

More generally, one can write

$$S(\nu) = \frac{2}{k_B T} \lim_{\tau \rightarrow \infty} \int_{-\tau}^{\tau} C(t) e^{-i2\pi\nu t} dt \quad (5)$$

where  $C(t)$  can be either the mass-weighted translational VACF determined from the center-of-mass velocity  $\mathbf{V}_i^{cm}(t)$  of the  $i^{th}$  water molecule,

$$C_T(t) = \sum_{i=1}^N \langle m_i \mathbf{V}_i^{cm}(t) \cdot \mathbf{V}_i^{cm}(0) \rangle \quad (6)$$

or the moment-of-inertia weighted angular velocity auto-correlation function

$$C_R(t) = \sum_{j=1}^3 \sum_{i=1}^N \langle I_{ij} \omega_{ij}(t) \omega_{ij}(0) \rangle \quad (7)$$

where  $I_{ij}$  and  $\omega_{ij}$  are, respectively, the  $j^{th}$  components of the moment of inertia tensor and the angular velocity of the  $i^{th}$  water molecule. Depending on the translational or rotational velocity correlation used in Eq.(5), one obtains the translational or rotational DoS.

In the 2PT method, the DoS is decomposed into a solid-like non-diffusive component and a gas-like diffusive component,  $S(\nu) = S^g(\nu) + S^s(\nu)$ , using the fluidity factor  $f$  which is a measure of the fluidity of system. The value of  $f$  is computed in terms of the dimensionless diffusivity  $\Delta$  using the *universal equation*<sup>13</sup>

$$2\Delta^{-9/2} f^{15/2} - 6\Delta^{-3} f^5 - \Delta^{-3/2} f^{7/2} + 6\Delta^{-3/2} f^{5/2} + 2f - 2 = 0. \quad (8)$$

The diffusivity  $\Delta$  can be uniquely determined for a thermodynamic state of the system using following equation:

$$\Delta(T, \rho, m, S_0) = \frac{2S_0}{9N} \left(\frac{6}{\pi}\right)^{2/3} \left(\frac{\pi kT}{m}\right) \rho^{1/3}, \quad (9)$$

where  $S_0 = S(0)$  is the zero-frequency component of the DoS function (translational or rotational). Knowing  $f$  from Eq.(8) and Eq.(9), the gas-like diffusive component of the DoS can be obtained using a hard-sphere diffusive model:

$$S^g(\nu) = \frac{S_0}{1 + \left[\frac{\pi s_0 \nu}{6fN}\right]^2}. \quad (10)$$

Lin *et al.*<sup>13</sup> used such a decomposition only for the translational DoS of monatomic fluids. In a recent development, Lin *et al.*<sup>18</sup> have shown that for polyatomic fluids, improved estimates of the rotational entropy can be obtained if such a gas-solid decomposition is used

for the rotational DoS as well. In this case, separate fluidity factors  $f$  are determined for the translational and rotational DoS using rotational and translational diffusivities in Eq.(8) and the gas-like component of entropy is determined by Eq.(10) with  $S_0$  being  $S_{tran}(0)$  or  $S_{rot}(0)$  for translational and rotational cases, respectively. Given such a DoS decomposition, every thermodynamic quantity has contributions from solid-like and gas-like DoS functions with appropriate weight functions:

$$A_m = \int_0^\infty d\nu S_m^g(\nu) W_{A,m}^g + \int_0^\infty d\nu S_m^s(\nu) W_{A,m}^s, \quad (11)$$

where  $m$  can be translational, rotational or vibrational. For the rigid water model used in our calculation, there is no contribution from intra-molecular vibrations. Details of the weight functions can be found in Ref.<sup>18</sup>. Different water models have been found to yield very accurate results for thermodynamic quantities over a large range of thermodynamics state points using this improved 2PT scheme.

### III. SIMULATION

We have performed a series of MD simulations of open-ended armchair SWCNTs immersed in a bath of water. We have used nanotubes of four different diameters, (5,5), (6,6), (7,7) and (8,8) having diameters of  $6.8\text{\AA}$ ,  $8.2\text{\AA}$ ,  $9.6\text{\AA}$  and  $10.9\text{\AA}$ , respectively. Interactions between various atoms were modeled by classical force-fields; carbon atoms were modelled as chargeless Lennard-Jones particles with  $sp^2$  hybridization (AMBER03 atom type ‘‘CA’’) with parameter values given in our earlier paper<sup>19</sup>. The equilibrium C-C bond length and the C-C-C angle were taken to be  $1.44\text{\AA}$  and  $2\pi/3$  respectively, with spring constants of  $938\text{Kcal/mol}/\text{\AA}^2$  and  $126\text{Kcal/mol}/\text{rad}^2$ , respectively. Water was modeled as a rigid molecule with the TIP3P potential. Electrostatic interactions were computed using the Particle Mesh Ewald (PME) method with a real space cutoff of  $10.5\text{\AA}$  and cubic B-spline interpolation. The same cut-off was used for Lennard-Jones interactions with a neighbor-list update frequency of 10. Each carbon nanotube had a length of  $56\text{\AA}$  with its axis fixed along  $z$ -axis during the whole simulation. The simulation unit box was created by solvating the carbon nanotube with  $15\text{\AA}$  water solvation shells in all three directions. Before using the MD trajectory for analysis, an energy minimization was done to remove bad contacts, followed by slow heating for 100 ps to reach the system temperature of 300K. The simulation box was

then equilibrated in the NPT ( $P = 1 \text{ atm}, T = 300\text{K}$ ) ensemble for at least 1 ns to get the correct density. Berendsen weak coupling method was used to maintain constant temperature and pressure with coupling constants of 0.5 ps and 0.2 ps, respectively, for temperature and pressure bath coupling. Finally, simulations were performed in the NVT ensemble with integration time-step of 1.0 fs. To compute the VACF, coordinates and velocity components of each atom were stored for 40 ps with 4 fs saving frequency. To get better statistical data, four independent trajectories were used for further computations. All the simulations reported here were done using the AMBER10<sup>20</sup> MD simulation package and visualization of simulation trajectories was done using VMD<sup>21</sup>.

To compute the entropy of bulk water, 100 water molecules, which remain at least  $10\text{\AA}$  away from the nanotube, were chosen at random. For confined water, only those water molecules which stay inside the tube during the complete production run were selected. Translational and rotational DoS were computed by decomposing the velocity into translational and rotational components at every step, computing velocity auto-correlation functions and taking their Fourier transform. The diffusivity of the system was computed using Eq.(9). This diffusivity was used to compute the fluidity factor  $f$  using Eq.(8). Knowing the fluidity factor  $f$ , the gas phase DoS was computed using Eq.(10) and the solid phase DoS was determined by subtracting the gas phase DoS from the total DoS. Note that such gas-solid decomposition was done for both translation and rotational DoS with fluidity factor computed separately for each case. The computed fluidity factors are given in Table I. Once we have this DoS decomposition, the entropy was computed using Eq.(11). The energy of each water molecule was computed by decomposing the potential energy per atom using MPSIM<sup>22</sup>. This decomposition was done by assigning equal values of energy to both atoms in the case of pair-wise interaction terms like the VDW energy and the bond energy. Long range Coulomb interaction energy of each atom was computed by observing that various terms in the Ewald energy are expressed in terms of the electrostatic potential at charge sites. Knowing the electrostatic potential at every charge site, the interaction energy of the  $i^{\text{th}}$  atom is the charge  $q_i$  multiplied by the potential at the site of the atom.



## IV. RESULTS

Translational and rotational VACFs are shown in Fig. 2 for water molecules in the bulk, as well as for those confined in (8,8), (7,7), (6,6) and (5,5) nanotubes. Fig. 3 and Fig. 4 show translational and rotational power spectra, respectively, for the same cases. Both translational and rotational VACFs in Fig. 2 show high-frequency oscillations for the water confined in narrow (5,5) and (6,6) nanotubes. These oscillations are more pronounced for (5,5) than for (6,6). The VACFs for water molecules confined in (7,7) and (8,8) nanotubes are similar to those of bulk water. Prominent peak appears in the translational power spectrum at  $121\text{cm}^{-1}$  for (5,5) and at  $47\text{cm}^{-1}$  for (6,6) nanotubes. For wider nanotubes, (7,7) and (8,8), where water molecules are not restricted to be arranged in single-file manner, the power spectrum (DoS function) is similar in shape to that of bulk water. We have observed a systematic variation of the position of this low-frequency peak with the diameter of the nanotube, as shown in Fig. 3.

In the case of bulk water, the low frequency peak around  $32\text{cm}^{-1}$  has been attributed to hindered translation in a local structural cage<sup>23</sup>. To find the molecular origin of the prominent peaks appearing in the DoS function of (5,5) and (6,6) nanotubes, we decomposed the translational velocity along longitudinal (parallel to the axis of the nanotube) and transverse (perpendicular to the nanotube axis) components and determined the DoS for motion in these two directions. Results shown in Fig. 5 suggest that the peak in Fig. 3 appears due to vibrational motion in direction perpendicular to axis of the nanotube. The confining potential is stronger in the case of the narrower (5,5) tube and hence the peak is blue shifted. For (7,7) and (8,8) nanotubes, water molecules have bulk-like environments and hence, they have DoS similar to that of bulk water with slight blue shift. Positions of these DOS peaks for translational modes have systematic variation with tube diameter as shown in the inset of Fig. 3. Similar behavior is also observed for the peak positions of the rotational DOS as shown in the inset of Fig. 4.

Due to single-file arrangement of water molecules inside (5,5) and (6,6) nanotubes, they have more freedom for rotational motion, and peaks in the rotational spectrum shift to lower frequencies as shown in Fig. 4. A distinct peak in the rotational DoS at  $146\text{cm}^{-1}$  is observed for water molecules confined in (6,6) nanotubes, whereas for the (5,5) nanotube, this peak appears to have merged with the zero-frequency diffusive peak. The emergence of

these peaks is a result of the change in the librational motion of water molecules when they are confined in narrow nanotubes. The reduction in the average number of hydrogen bonds per water molecule from 4 in the bulk to 2 for single-file water in narrow nanotubes leads to less constrained rotation and faster rotational diffusion of water molecules inside these nanotubes.

Table I gives a summary of the results of our entropy calculations. For bulk water, the calculated total (translational plus rotational) entropy is 4.95 Kcal/mol for  $T = 300\text{K}$  which is quite close to the experimental value of 5.01 Kcal/mol<sup>24</sup> under the same conditions. This value is also close to the results obtained from a recently developed methods based on cell theory<sup>24</sup> which also uses the harmonic approximation for calculating the entropy, as in the 2PT method. This gives us confidence that the rotational entropy of water molecules obtained from the 2PT method is accurate enough to explain the thermodynamics of entry of water inside the hydrophobic pores of nanotubes. Here we would like to clarify that the number of water molecules inside the nanotube is not constant during the simulation. Hence the values of  $\langle E \rangle$  and  $\langle S \rangle$  reported here correspond to averages in the grand canonical ensemble. Therefore,  $A = \langle E \rangle - T \langle S \rangle$  is not the canonical Helmholtz free energy, here onwards we represents  $\langle E \rangle$ ,  $\langle S \rangle$ ,  $A$  by  $\langle E \rangle^{GC}$ ,  $\langle S \rangle^{GC}$  and  $A^{GC}$  to indicate that these values belong to grand canonical ensemble for confined water. Note that this difference between the this free energy and the conventional canonical Helmholtz free energy will be of the negligible when the number of particles in the nanotube is very large<sup>25</sup>. This however is not the case as the number of particles inside nanotube in our case is around 20. It may be pertinent to remark that the calculation of Helmholtz free energy for the water molecules inside the nanotube is done by Vaitheeswaran *et. al.*<sup>6</sup> is for a fixed number of water molecules inside the nanotube, hence the relation used there (Eq. 16 of ref. 6) is not valid in our case.

From Table I, we see that for water inside nanotubes, when the diameter of the nanotube is so small that there is only a single chain of water molecules inside the nanotube (i.e. for (5,5) and (6,6) nanotubes), the rotational entropy is substantially higher in comparison to the value of 0.97 kcal/mol for bulk water. There is a 70-120% increase in the rotational component of the entropy for the confined water molecules compared to that in the bulk. This increase in rotational entropy is due to unhindered rotation of the dipole vector in the absence of a three-dimensional network of hydrogen bonds that is present in the bulk. Due

to single file arrangement of water inside nanotubes, each water molecule can rotate freely in such a way that the component of the dipole moment of every confined water molecule along the nanotube axis remains nearly constant, while the azimuthal component relaxes very fast, providing more rotational freedom. The resulting gain in rotational entropy helps to compensate the energy cost due to the loss of hydrogen bonds inside a nanotube, as well as the loss in translational entropy. Because of this compensation, the free energy  $A^{GC}$  per water molecule inside (6,6), (7,7), and (8,8) nanotubes is the same as that for bulk water within the accuracy of our calculation. [Vaitheeswaran \*et. al.\*<sup>6</sup> have computed free energy of transfer and found similar entropy gain for water molecules inside nanotube for occupancy of 5 for 14Å long tube but they have observed that it is energetically favourable for water molecules to be inside hydrophobic channel which is quite against to the intuition. Change in energy is correctly captured in our calculation which reveals energy loss inside nanotube.](#)

The Helmholtz free energy per water molecule inside a (5,5) nanotube is around 1 kcal/mol higher than that in bulk water. In spite of this higher free energy, water spontaneously enters inside (5,5) nanotube. To have a microscopic understanding of this phenomenon, we have performed very long simulations (total duration of 100 ns) for (5,5) and (6,6) nanotubes of length 13.4 Å immersed in water and found that for the (5,5) nanotube, there are many emptying transitions when there are no water molecules inside the nanotube. In fact, for the 100 ns long simulation, the nanotube remains empty for almost 13 ns, which is 13% of the simulation time (see Fig. 6). In contrast, for the (6,6) nanotube, there are always at least 2 water molecules inside the nanotube in a 100 ns simulation run. In Fig. 7, we plot the occupation probability of water molecules for (5,5) and (6,6) nanotubes. In the case of the (6,6) nanotube, the occupancy is peaked at 5 water molecules (see Fig. 7) while the (5,5) nanotube has considerable weights for smaller numbers of water molecules due to the occurrence of many emptying transitions. This is consistent with the results of our free energy calculation. Water molecules may enter a (5,5) nanotube due to thermal fluctuations even if the free energy of a water molecule inside the nanotube is higher than that in the bulk. However, the higher free energy of a water molecule inside a (5,5) nanotube results in a reduction in the average occupation of the nanotube by water molecules in long simulations. Interestingly, we find that the probability of the durations during which the (5,5) nanotube remains empty can be fitted to an exponential distribution, as shown in the inset of Fig. 7.

To check the presence of finite-size effects in our entropy calculations, we have carried

out these computations for three different lengths of tubes (20, 40, and 60 unit cells) and found the same value of the entropy in all three cases.

## V. CONCLUSION

We have shown that water molecules have significant gain in rotational entropy when they come inside narrow carbon nanotubes. This gain is considerable for the narrower tubes for which water molecules inside the tube form single-file chains. For such tubes, the gain in rotational entropy compensates the increase in energy due to a reduction in the number of hydrogen bonds per water molecule, so that the average free energy of a water molecule inside the tube is the same (except for the narrowest (5,5) tubes) as that in the bulk. This explains the observation that water goes inside narrow carbon nanotubes in spite of the hydrophobic nature of the cavity. As the diameter of the tube increases, entropy and energy values approach those of bulk water. We have also observed considerable shifts in the peaks of the DoS functions which might serve as spectroscopic signatures of the confined water.

## VI. ACKNOWLEDGMENT

We thank DST, India for financial support. HK would like to thank University Grants Commission, India for Junior Research Fellowship.

## REFERENCES

- <sup>1</sup>G. Hummer, J. C. Rasaiah, J. P. Noworyta, *Nature*, 414, 188(2001).
- <sup>2</sup>K. Koga, G. T. Gao, H. Tanaka, X. C. Zeng, *Nature*, 412, 802(2001).
- <sup>3</sup>L. Maibun, D. Chandler, *J. Phys. Chem. B*, 107, 1189-1193, 2003.
- <sup>4</sup>X. Zhou, C. Quan Li, M. Iwamoto, *J. Chem. Phys.*, 121, 7996, 2004.
- <sup>5</sup>J. C. Rasaiah, S. Gadre, G. Hummer, *Ann. Rev. Phys. Chem.*, 59, 713-40 2008.
- <sup>6</sup>S. Vaitheeswaran, J. C. Rasaiah, G. Hummer, *J. Chem. Phys.*, 121, 7955, 2004.
- <sup>7</sup>M. Majumder, N. Chopra, R. Andrews, B. J. Hinds, *Nature*, 438, 44(2005).
- <sup>8</sup>A. I. Kolesnikov, J. M. Zanotti, C. K. Loong, P. Thiyagarajan, A. P. Moravsky, R. O. Loutfy, C. J. Burnham, *Phys. Rev. Lett.*, 93, 035503(2004).
- <sup>9</sup>B. Mukherjee, P. K. Maiti, C. Dasgupta, A. K. Sood, *ACS Nano*, 2, 1189(2008).

- <sup>10</sup>R.B. Best, G. Hummer, Proc. Natl. Acad. Sci. U.S.A., 102, 6732(2005).
- <sup>11</sup>B. Mukherjee, P. K. Maiti, C. Dasgupta, A. K. Sood, J. Phys. Chem. B , 113, 10322(2009).
- <sup>12</sup>D. Laage, J. T. Hynes, Science, 311, 832(2006).
- <sup>13</sup>S. T. Lin, M. Blanco, W. A. Goddard, J. Chem. Phys., 119, 11792(2003).
- <sup>14</sup>S. T. Lin, P. K. Maiti, W. A. Goddard, J. Phys. Chem. B, 109, 8663(2005).
- <sup>15</sup>S. T. Lin, S. S. Jang, T. Cagin, W. A. Goddard, J. Phys. Chem. B, 108, 10041(2004).
- <sup>16</sup>B. Jana, S. Pal, P. K. Maiti, S. T. Lin, J. T. Hynes, B. Bagchi, J. Phys. Chem. B , 110, 19611(2006).
- <sup>17</sup>A. A. McQuarrie, Statistical Mechanics (Harper & Row, New York, 1976).
- <sup>18</sup>S. T. Lin, P. K. Maiti, W. A. Goddard, J. Phys. Chem. B, 114, 8191(2010).
- <sup>19</sup>B. Mukherjee, P. K. Maiti, C. Dasgupta, A. K. Sood, J. Chem. Phys., 126, 124704(2007).
- <sup>20</sup>D. A. Case, T. A. Darden, T. E. Cheatham, C. L. Simmerling, *et. al*, AMBER10(University of California, San Francisco).
- <sup>21</sup>W. Humphrey, A. Dalke, K. Schulten, J. Molec. Graphics, 14.1, 33(1996).
- <sup>22</sup>K. T. Lim, S. Brunett, M. Lotov, *et. al*, J. comput. chem., 18, 501 (1997).
- <sup>23</sup>J. A. Padro, J. Marti, J. Chem. Phys., 118, 452(2001).
- <sup>24</sup>NIST Chemistry Webbook, NIST Standard Reference Database number 69, June (2005) release, <http://webbook.nist.gov/chemistry/>
- <sup>25</sup>*It can be shown value of  $\langle E \rangle - T \langle S \rangle$  calculated in grand canonical ensemble( computed for  $\langle N \rangle$ ) and canonical ensemble will be equal for very large values of  $N$  because of striling approximation involved in ensemble transformation, which is valid only for large value of  $N$ .*

## FIGURES

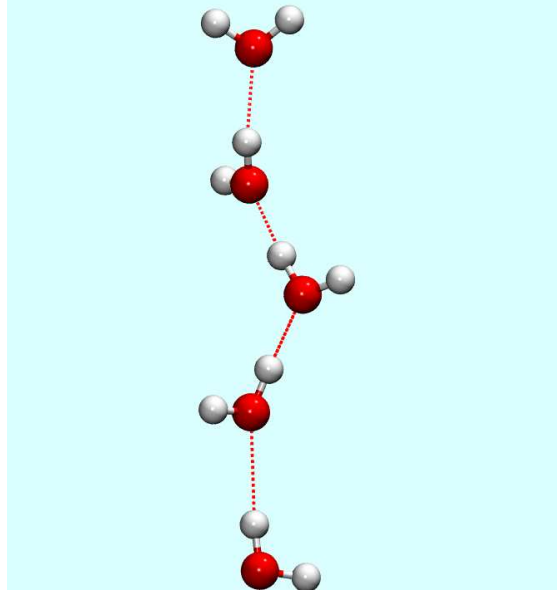


FIG. 1. Single-file arrangement of water molecules inside a (6,6) nanotube. One of the hydrogen atoms of each water molecule is not hydrogen-bonded and hence, the corresponding OH vector can rotate freely.

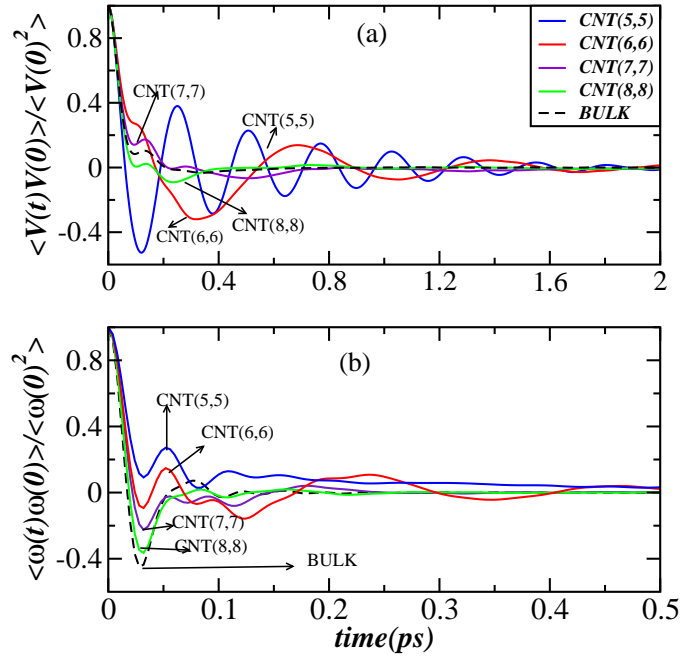


FIG. 2. Translational (a) and rotational (b) velocity auto-correlation functions of water molecules in the bulk and of those confined inside (8,8), (7,7), (6,6), and (5,5) nanotubes of length  $54\text{\AA}$ , calculated at  $T = 300\text{K}$ .

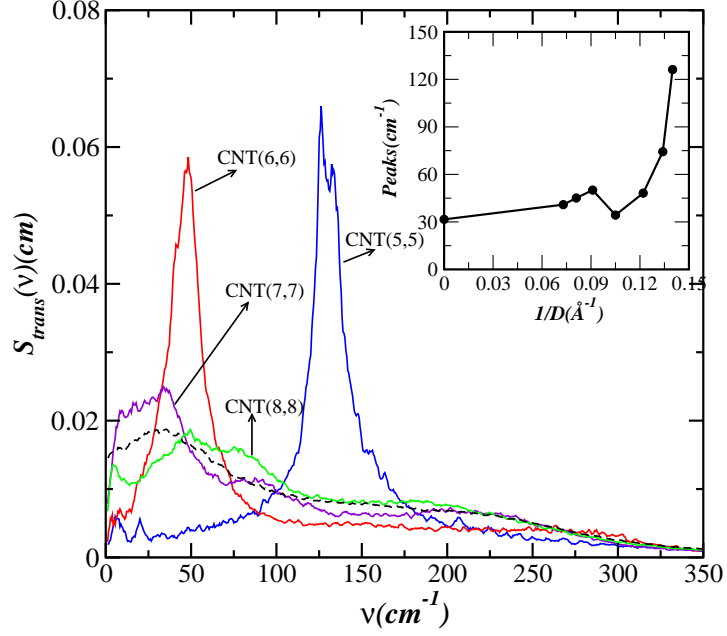


FIG. 3. Translational DoS function of water molecules in the bulk and of those confined inside (8,8), (7,7), (6,6) and (5,5) nanotubes of length  $54\text{\AA}$ , calculated at  $T = 300\text{K}$ . Note the gradual shift in the peak frequencies as the diameter of the tube is increased. The inset shows the variation of the peak position with the inverse of the tube diameter.

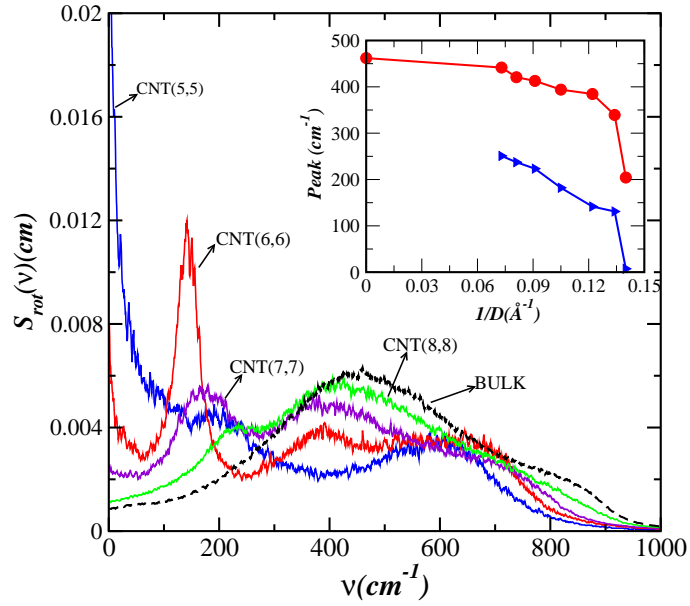


FIG. 4. Comparison of rotational DoS of water molecules in the bulk and of those confined inside (8,8), (7,7), (6,6), and (5,5) nanotubes of length  $54\text{\AA}$ , calculated at  $T = 300\text{K}$ . The inset shows the dependence of the peak positions on the inverse of the tube diameter. Triangles ( $\triangleright$ ) denote the positions of the first peak and circles ( $\bullet$ ) denote the positions of the second peak of the rotational DoS.

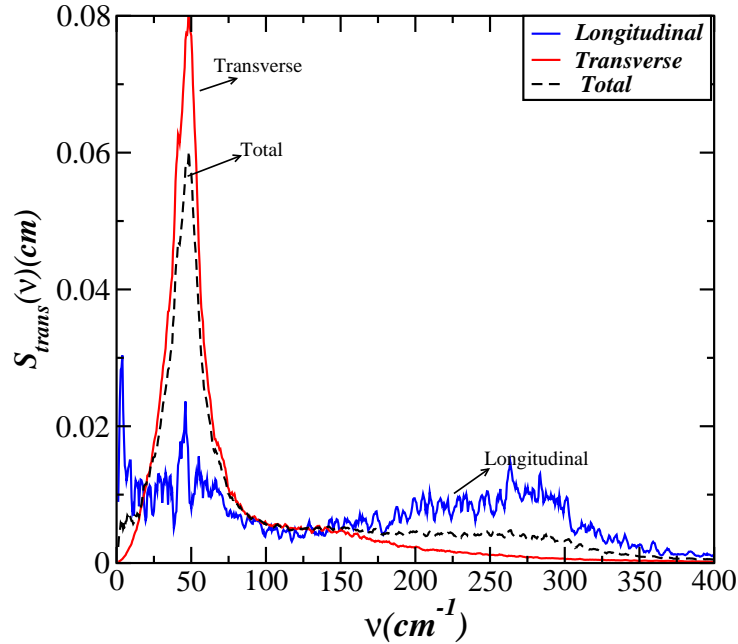


FIG. 5. Decomposition of the translational DoS function in longitudinal and transverse directions for water in a (6,6) nanotube of length  $54\text{\AA}$ , calculated at  $T = 300\text{K}$ . It is obvious that the peaks in the DoS arise from transverse motion.



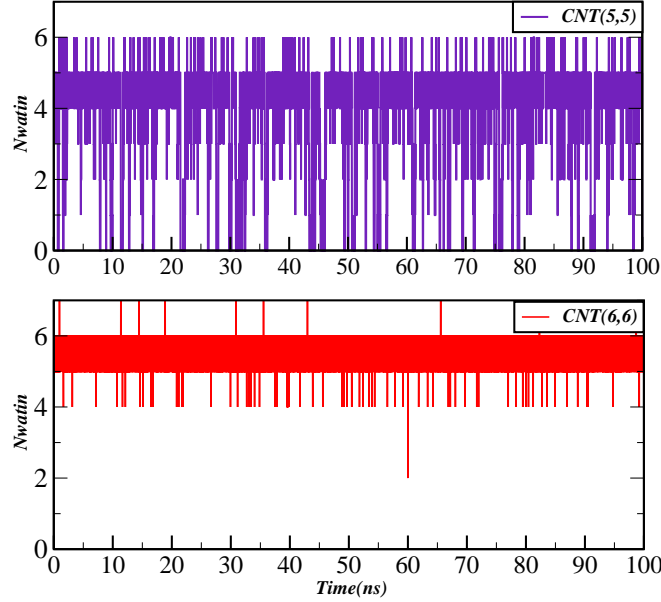


FIG. 6. Number of water molecules inside 13.4 Å long (5,5) (top panel) and (6,6) (bottom panel) nanotubes as function of time at  $T = 300\text{K}$ . During 100 ns of simulation time, the (5,5) nanotube have many instances when there is no water inside the tube, while inside the (6,6) nanotube, at least four water molecules are always present (except once). This is consistent with the computed free energy values.

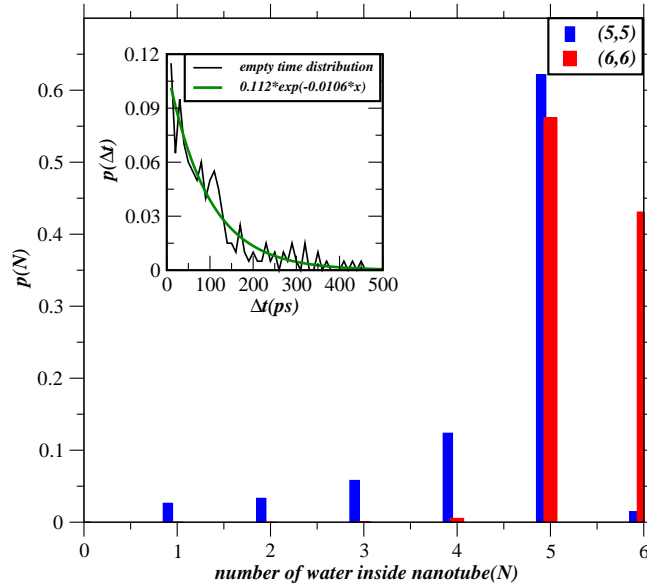


FIG. 7. Probability of having a particular number of water molecules inside 13.4 Å long (5,5) and (6,6) nanotubes at  $T = 300\text{K}$ . The inset shows the probability distribution of time intervals during which the (5,5) nanotube remains empty, fitted to an exponential function.

## TABLES

	$\langle E \rangle^{GC}$ <sup>a</sup>	$T \langle S_{trans} \rangle^{GC}$	$T \langle S_{rot} \rangle^{GC}$	$A^{GC}$	$f_{trans}$ <sup>b</sup>	$f_{rot}$ <sup>b</sup>
(5, 5)	$-8.26 \pm (0.20)$	$2.97 \pm (.20)$	$2.16 \pm (0.18)$	$-13.39 \pm (0.58)$	$0.12 \pm (.04)$	$0.42 \pm (.03)$
(6, 6)	$-8.89 \pm (0.20)$	$3.84 \pm (.20)$	$1.67 \pm (0.15)$	$-14.40 \pm (0.55)$	$0.15 \pm (.04)$	$0.30 \pm (.03)$
(7, 7)	$-8.67 \pm (0.20)$	$4.04 \pm (.10)$	$1.42 \pm (0.07)$	$-14.13 \pm (0.37)$	$0.17 \pm (.01)$	$0.15 \pm (.03)$
(8, 8)	$-9.38 \pm (0.10)$	$3.67 \pm (.10)$	$1.12 \pm (0.07)$	$-14.17 \pm (0.27)$	$0.20 \pm (.02)$	$0.10 \pm (.01)$
<i>BULK</i>	$-9.45 \pm (0.02)$	$4.02 \pm (.05)$	$0.93 \pm (0.01)$	$-14.40 \pm (0.08)$	$0.34 \pm (0.005)$	$0.08 \pm (.004)$

<sup>a</sup> In Kcal/mol

<sup>b</sup> Fluidity factor

<sup>c</sup> Superscript GC indicates that values quoted here belongs to Grand canonical ensemble for confined water molecules.

TABLE I. The energy, entropy and free energy per water molecule( $A^{GC} = \langle E \rangle^{GC} - T \langle S \rangle^{GC}$ ) in Kcal/mol and fluidity factors at  $T = 300\text{K}$  for the water molecules confined in  $54\text{\AA}$  long tubes of various diameters and for bulk water calculated in NVT ensemble.